Sensors and Materials, Vol. 34, No. 5 (2022) 1721–1731
MYU Tokyo

S & M 2923

Using Overall Transfer Matrix to Simulate a Blue-light Bragg Reflector with Optimization Properties

Yonghu Yang,[1] Jin-Yu Chen,[2] Cheng-Fu Yang,[2,3*]
Chang Hong Lin,[2] and Chiang-Lung Lin[1**†]

[1]Dongguan City College, Guangdong 523419, P.R. China
[2]Department of Chemical and Materials Engineering, National University of Kaohsiung, Kaohsiung 811, Taiwan
[3]Department of Aeronautical Engineering, Chaoyang University of Technology, Taichung 413, Taiwan

(Received December 30, 2021; accepted March 23, 2022)

Keywords: blue-light Bragg reflector, simulation, overall transfer matrix, MgF_2-Nb_2O_5 bilayer film, different thicknesses

In this study, an e-beam evaporation method was used to deposit Nb_2O_5 and MgF_2 single-layer films on glass substrates; then, the refractive indexes (n values) of the glass substrate and Nb_2O_5 and MgF_2 single-layer films were measured in the range of 200–1700 nm. The equation $d = \lambda/(4n)$ was used to determine the thicknesses (d) of the two films with 1/4 wavelength (λ), which were used in a distributed Bragg reflector (DBR) with the central wavelength of ~450 nm (blue light). The calculated thicknesses of the Nb_2O_5 and MgF_2 single-layer films were 49.0 and 80.9 nm, respectively. The measured refractive indexes of the Nb_2O_5 and MgF_2 single-layer films were incorporated into an approximate equation proposed by Sheppard to measure the maximum reflective ratios (MaxR) of the blue-light DBRs with different periods (two, four, and six were investigated in this study). Also, an overall transfer matrix (TM) was investigated to calculate the simulative reflective spectra of the blue-light DBRs with two, four, and six periods. The TM of each layer with the same thickness was obtained by changing the thicknesses of the MgF_2 film from 76.9 to 84.9 nm (the thickness of the Nb_2O_5 film was set at 49.0 nm) and those of the Nb_2O_5 film from 45.0 to 53.0 nm (the thickness of the MgF_2 film was set at 80.9 nm). The effects of the variations in the thicknesses of the Nb_2O_5 and MgF_2 films on the simulated reflective spectra of the designed blue-light DBRs were well investigated. The measured MaxR values were also compared with the results calculated using the equation proposed by Sheppard, because it can only be used to calculate the MaxR value of a designed DBR.

1. Introduction

Multilayer films of nanometer scale can have specific properties, and when they are constructed with different materials, they can have a wide range of applications because of their outstanding protective, photoactive, and optical properties. For example, a highly reflective distributed Bragg reflector (DBR) can be used to construct a microcavity with exciton-polarization to achieve semiconductive lasers with a long lifetime.[1,2] A DBR is designed to

*Corresponding author: e-mail: cfyang@nuk.edu.tw
**Corresponding author: e-mail: chlulin0510@gmail.com
†Present address: College of Art, Zhongqiao Vocational and Technical University, Shanghai 201514, China

https://doi.org/10.18494/SAM3818
ISSN 0914-4935
https://myukk.org/

reflect light with a specific wavelength and a narrow bandwidth, and it can also be used to fabricate a notch filter.[3] DBRs are constructed from multiple layers of different materials with varying refractive indexes in the vertical direction (*n* values; films with high and low *n* values are alternately stacked), and the thicknesses of these films are at a quarter-wave (λ/4) of the designed reflective wavelength. Bilayer-film designs can be found in commercial wavelength division multiplexers, which have single-period structures of H(TiO_2)/L(Al_2O_3), H(TiO_2)/L(SiO_2), H(Nb_2O_5)/L(SiO_2), or H(Ta_2O_5)/L(SiO_2) and use different numbers of periods.[4–6]

The DBRs can be used in the grating technology of fiber Bragg filters; they are also popularly applied in sensors for different physical measurements, such as temperature, strain, and pressure, which are applied in the industrial engineering, aerospace, maritime, and civil engineering fields.[7] For example, the applications of DBRs in a fiber grating interrogator can enable the integration of a broad-band light source and a photodetector to fabricate a small, high-precision, and continuous plethysmograph monitoring system.[7] Many methods are investigated to design a multilayer DBR with optimal properties. For example, COMSOL Multiphysics® (abbreviated as COMSOL) is a very useful simulation tool that can simulate and analyze the optical and electromagnetic properties of materials with different structures. Previously, we successfully used COMSOL to design a multilayer red DBR with optimal reflection properties.[7] When COMSOL is used to design a red DBR, we can easily obtain the optimal thicknesses of deposited multilayer films by changing the sampling space and setting the intensities to obtain the DBR in the passband having a small FWHM, low ripple intensities, and high reflectance, and small ripple intensities outside of the reflectance band. Previously, we deposited SiO_2-Nb_2O_5 bilayer films with different periods on glass substrates to fabricate a DBR with the central wavelength (nm, CWave, defined as the central wavelength of the bandwidth) of 450 nm.[8] An overall transfer matrix (TM) was constructed to calculate and simulate the reflectance properties by incorporating various *n* values and thicknesses of each layer of different films. We found that the properties of the simulated reflectance spectra matched the measured results of the fabricated DBRs. However, there are no research studies that used an overall TM to determine the effect of the variations in the thicknesses of the used films on the reflectance properties of the designed DBRs. Therefore, we investigated and used an overall TM to determine when the thicknesses of the used films were changed, and the variations in the reflectance properties of the designed 450 nm DBR were investigated

Previously, Du *et al*. used bilayer Nb_2O_5 and MgF_2 films to design a DBR with a central wavelength of 500 nm.[9] However, they only used an e-beam to deposit the bilayer Nb_2O_5 and MgF_2 films and measured their reflectance spectra. In this study, two reasons motivated us to use Nb_2O_5 and MgF_2 films for the fabrication of the multiperiod reflective films having an L (MgF_2, 1/4 λ)/H (Nb_2O_5, 1/4 λ) bilayer structure. The first is that the difference in the *n* values of the Nb_2O_5 film (n ~ 2.30 in visible light)[10] and the MgF_2 film (n ~1.39 in the light range of 400–700 nm)[11] is large. The second is that the *k* values of both Nb_2O_5 and MgF_2 films are low in the range of visible light.[10,11] In this paper, we show that even for the MgF_2-Nb_2O_5 bilayer films with only four periods, the designed DBRs have a reflective ratio of more than 90%. To investigate the effect of the variations in the thicknesses of the Nb_2O_5 and MgF_2 films on the potential changes of the designed blue-light DBRs with different periods, we performed the

following steps. First, the single-layer Nb_2O_5 and MgF_2 films were deposited on glass substrates, and their n values were measured; therefore, the thicknesses of the $\lambda/4$ Nb_2O_5 and MgF_2 films were obtained. Second, a characteristic overall TM for simulating the multilayer films was investigated and used to calculate the reflective properties of the bilayer MgF_2-Nb_2O_5 DBRs with different periods by incorporating the optical parameters of the single-layer Nb_2O_5 and MgF_2 films.

An approximate equation proposed by Sheppard is used to determine the variations in the maximum reflective ratios of multilayer MgF_2-Nb_2O_5 DBRs versus the variations in period numbers:[12]

$$R = \left[\frac{(n_H)^{2P} - (n_0 / n_S) \times (n_L)^{2P}}{(n_H)^{2P} + (n_0 / n_S) \times (n_L)^{2P}} \right]^2, \quad (1)$$

where n_S, n_H, n_L, and n_0 are the refractive indexes of the glass substrate (n_S = 1.52), Nb_2O_5 (n_H = 2.29), MgF_2 (n_L = 1.39), and air (n_0 = 1), respectively, R is the maximum reflective ratio at a special wavelength of light, and P is the period of the designed MgF_2-Nb_2O_5 DBR. However, Eq. (1) is only used to calculate the maximum reflective ratio (MaxR) of the designed DBR at a special wavelength, and it cannot simulate the reflective spectrum in a very wide range of light wavelength. Previously, as the equation $d = \lambda/(4n)$ was used to calculate the thicknesses of the used films, the obtained thicknesses were recognized as the optimal values to design a DBR at a specific wavelength, where d, λ, and n are the thickness, targeted wavelength, and refractive index of the used films, respectively. However, to the best of our knowledge, there is no study on the effect of thickness variation on the reflective spectra of a designed DBR. The important novelty of this study is that we investigated an overall TM that we proposed to simulate the reflective spectra of a designed DBR at a CWave of 450 nm. Then, layers with the same thicknesses were incorporated into the matrix by changing the thickness of the MgF_2 film from 76.9 to 84.9 nm (the thickness of the Nb_2O_5 film was set at 49.0 nm) and those of the Nb_2O_5 film from 45.0 to 53.0 nm (the thickness of the MgF_2 film was set at 80.9 nm). Finally, we discussed the effects of different thicknesses on the reflective spectra of the designed DBR and compared the MaxR values obtained from the approximate equation proposed by Sheppard and from the investigated overall TM.

2. Simulation Process and Parameters Used

To use the Nb_2O_5 and MgF_2 films as the high- and low-n-value films, respectively, in the design of a multilayer blue-light DBR on Corning 1737 glass substrates, their refractive indexes were measured first. An e-beam was used to deposit the Nb_2O_5 and MgF_2 single-layer films on Corning 1737 glass substrates to measure their n values; the relative parameters to deposit the Nb_2O_5 and MgF_2 films are given in Ref. 9. The thicknesses of the deposited Nb_2O_5 and MgF_2 films were 58.4 and 57.7 nm, respectively, and an N&K analyzer was used to measure their n values. For designed MgF_2-Nb_2O_5 DBRs, a MgF_2 film was deposited on a glass substrate and a

Nb_2O_5 film was deposited on the MgF_2 film, as Fig. 1 shows, and one period of the MgF_2-Nb_2O_5 bilayer film was formed. In this study, we used two, four, and six periods to design the DBRs.

Because light is a type of electromagnetic wave, for a single-layer film on a substrate and in air, when we used a and b to denote the interfaces between the film and air and between the substrate and film. The formulas of amplitude reflection (ρ) and transmission (τ) coefficients are expressed as [13,14]

$$\rho = \frac{E_{0a}^{-}}{E_{0a}^{+}} = \frac{\eta_0 E_a - H_a}{\eta_0 E_a + H_a} \text{ and } \tau = \frac{E_b}{E_{0a}^{+}} = \frac{2\eta_0 E_b}{\eta_0 E_a + H_a}. \tag{2}$$

Therefore, the relationship between electrical field (E_a) and magnetic field (H_a) is written in the matrix equation[13,14]

$$\begin{bmatrix} E_a \\ H_a \end{bmatrix} = \begin{bmatrix} \cos\delta & \frac{i}{N}\sin\delta \\ iN\sin\delta & \cos\delta \end{bmatrix} \begin{bmatrix} E_b \\ H_b \end{bmatrix}, \tag{3}$$

where δ is the phase factor and it is shown as

$$\delta = 2\pi\, Nd\cos(\theta)/\lambda, \tag{4}$$

where N is the complex index and it is equal to ($nr - ikr$). n, k, d, and λ are the refractive index, extinction coefficient, film thickness, and light wavelength, respectively. For the deposited film, N is defined as its modified optical admittance, and it is shown as

$$N = \vec{E}/\vec{H}. \tag{5}$$

When light propagates in a multilayer film from the front face of a reference plane (often air) to the surface of a multilayer film, and then to the substrate, the variations of the input optical

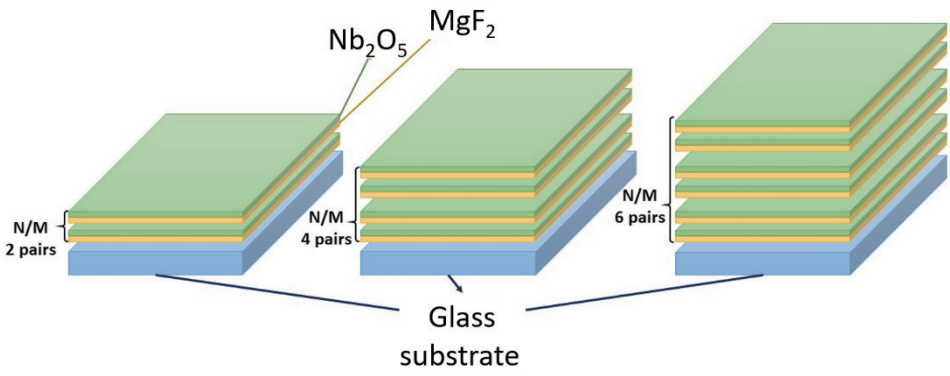

Fig. 1. (Color online) Structure of designed MgF_2-Nb_2O_5 DBRs with different periods.

admittance for single-layer, two-layer (one period, $P = 1$), four-layer ($P = 2$), eight-layer ($P = 4$), and twelve-layer ($P = 6$) structures are as follows:

$$\begin{bmatrix} B_1 \\ C_1 \end{bmatrix} = \begin{bmatrix} \cos\delta_1 & \frac{i}{N}\sin\delta_1 \\ iN\sin\delta_1 & \cos\delta_1 \end{bmatrix} \begin{bmatrix} 1 \\ y_s \end{bmatrix}, \; Y_1 = \frac{B_1}{C_1}, \tag{6}$$

$$\begin{bmatrix} B_2 \\ C_2 \end{bmatrix} = \begin{bmatrix} \cos\delta_2 & \frac{i}{N}\sin\delta_2 \\ iN\sin\delta_2 & \cos\delta_2 \end{bmatrix} \begin{bmatrix} 1 \\ Y_1 \end{bmatrix}, Y_2 = \frac{B_2}{C_2}, \tag{7}$$

$$\begin{bmatrix} B_4 \\ C_4 \end{bmatrix} = \begin{bmatrix} \cos\delta_4 & \frac{i}{N}\sin\delta_4 \\ iN\sin\delta_4 & \cos\delta_4 \end{bmatrix} \begin{bmatrix} 1 \\ Y_3 \end{bmatrix}, \; Y_4 = \frac{B_4}{C_4}, \tag{8}$$

$$\begin{bmatrix} B_8 \\ C_8 \end{bmatrix} = \begin{bmatrix} \cos\delta_8 & \frac{i}{N}\sin\delta_8 \\ iN\sin\delta_8 & \cos\delta_8 \end{bmatrix} \begin{bmatrix} 1 \\ Y_9 \end{bmatrix}, \; Y_8 = \frac{B_8}{C_8}, \tag{9}$$

$$\begin{bmatrix} B_{12} \\ C_{12} \end{bmatrix} = \begin{bmatrix} \cos\delta_{12} & \frac{i}{N}\sin\delta_{12} \\ iN\sin\delta_{12} & \cos\delta_{12} \end{bmatrix} \begin{bmatrix} 1 \\ Y_{11} \end{bmatrix}, Y_{12} = \frac{B_{12}}{C_{12}}, \tag{10}$$

$$R = |\rho|^2 = \frac{|Y_0 - Y_4|^2}{|Y_0 + Y_4|^2} \text{ for } P = 2, \; R = |\rho|^2 = \frac{|Y_0 - Y_8|^2}{|Y_0 + Y_8|^2} \text{ for } P = 4,$$

$$R = |\rho|^2 = \frac{|Y_0 - Y_{12}|^2}{|Y_0 + Y_{12}|^2} \text{ for } P = 6, \tag{11}$$

where y_s is the admittance of the substrate.

3. Simulation Results and Discussion

The measured n values of the single-layer Nb_2O_5 and MgF_2 films and glass substrate as a function of light wavelength are shown in Fig. 2(a). Apparently, the n value of the Nb_2O_5 film is larger than those of the MgF_2 film and glass substrate in all measured wavelengths. Therefore, the Nb_2O_5 film was used as a high-n-value film and the MgF_2 film was used as a low-n-value film to design a multilayer blue-light DBR. As Fig. 2(a) shows, the n value of the Nb_2O_5 film was 2.52 at 350 nm, and it critically decreased as the light wavelength increased. As the light wavelength increased from 400 to 500 to 700 nm, the n values decreased from 2.38 to 2.23 to

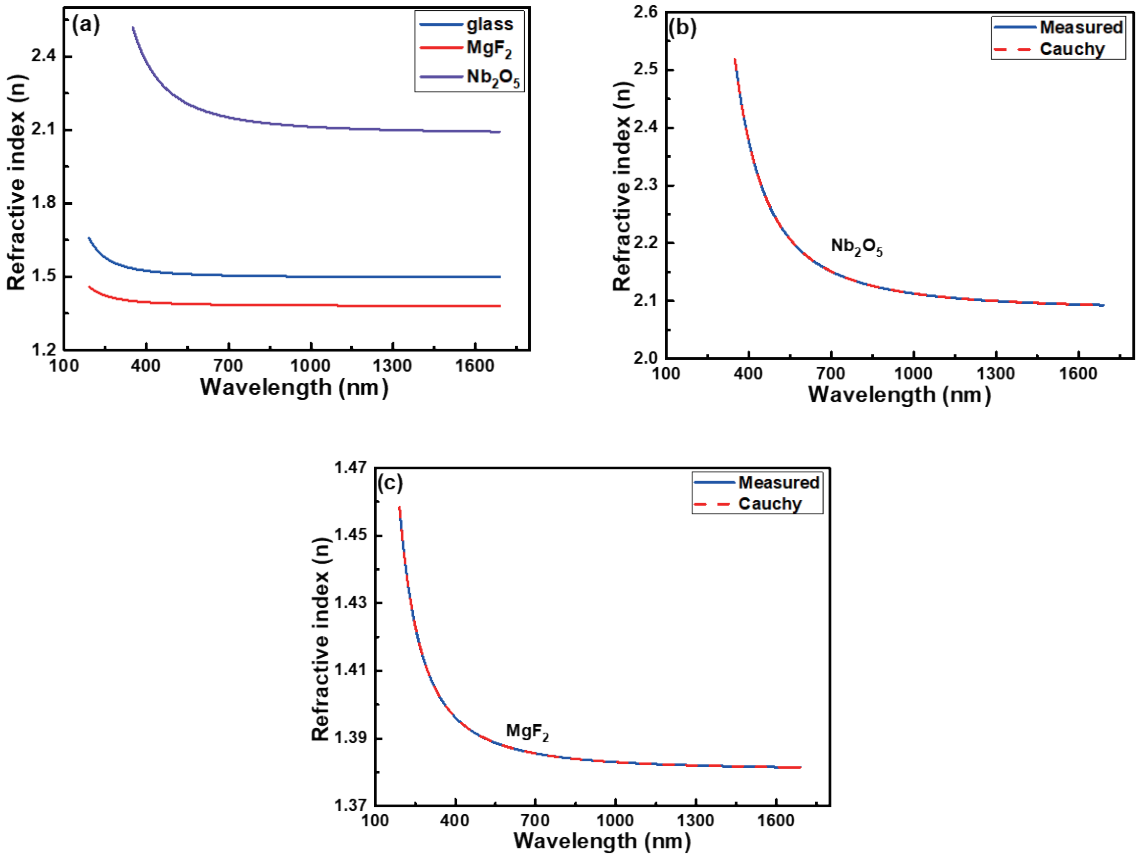

Fig. 2. (Color online) (a) Measured n values of single-layer Nb_2O_5 and MgF_2 films and glass substrate; (b) and (c) n values of Nb_2O_5 and MgF_2 single-layer films given with the simulation results using Cauchy's equation.

2.15. However, when the light wavelength of the Nb_2O_5 film was larger than 750 nm, its n value showed no apparent change. The MgF_2 film had an n value of 1.45 at 200 nm; the n value decreased slightly as the light wavelength became larger and were 1.41 and 1.40 at the light wavelengths of 300 and 400 nm, respectively. Also, the glass substrate had n values of 1.64, 1.55, and 1.52 at the light wavelengths of 200, 300, and 400 nm, respectively. As the light wavelengths further increased to more than 400 nm, the n values of the MgF_2 film and glass substrate became stable. Because we wanted to design an optical reflector with a CWave of blue light (450 nm), we chose n values of 2.29 and 1.39 (both at 450 nm) for the Nb_2O_5 and MgF_2 films, respectively. Next, the equation $d = \lambda/(4n)$ was used to calculate the thicknesses of the Nb_2O_5 and MgF_2 films that matched the designed wavelength of DBRs (450 nm). From the calculation of $d = \lambda/(4n)$, the thicknesses of 49.1 and 80.9 nm were matched with the thicknesses of the Nb_2O_5 and MgF_2 films under the $\lambda/4$ condition, respectively.

However, the n value of the MgF_2 film decreased quickly with the wavelength in the range of 200–500 nm, and the n value of the Nb_2O_5 film decreased rapidly with the wavelength in the range of 200–700 nm. Many factors will cause the decrease in the n value with the light wavelength, such as the extinction coefficient and normal dispersion of the materials or films used. Cauchy investigated a transmission equation to present an empirical relationship between

the light wavelength and the n value for the transparent material or film, as explained in Ref. 15. The most general form of Cauchy's investigated equation in the visible wavelength range is

$$n(\lambda) = a + b/\lambda^2 + c/\lambda^4 + \ldots, \tag{12}$$

where λ and n are the measured wavelength and the n value of the transparent film or material used, respectively, and a, b, and c, are the coefficients used to determine the parameters in the equation. The coefficients are usually measured in μm and quoted for λ as the vacuum wavelength in a material. Typically, an at least three-term form of the equation, as the following form shows, is sufficient to express a material:

$$n(\lambda) = a + b/\lambda^2 + c/\lambda^4. \tag{13}$$

For the Nb_2O_5 film, the c, b, and a values are 3.2799308×10^{-3} (μm^4), 2.6614043×10^{-2} (μm^2), and 2.0830535, and for the MgF_2 film, the c, b, and a values are 1.6955936×10^{-5} (μm^4), 2.3938716×10^{-3} (μm^2), and 1.3805820, respectively. Apparently, as Figs. 2(b) and 2(c) show, when Eq. (13) is used to calculate the n values and the wavelengths are different, the calculated values match the variations in the measured values of the Nb_2O_5 and MgF_2 films. Those results prove that for the Nb_2O_5 and MgF_2 single-layer films, the decreases in their n values are caused by the normal dispersions of the Nb_2O_5 and MgF_2 films, and they are not caused by their extinction properties.

Because the decreases in the n values of the Nb_2O_5 and MgF_2 single-layer films are caused by their normal dispersion, the variations of the n values shown in Fig. 2(a) are used to simulate the reflective spectra of the designed DBRs shown in Fig. 1. When the thicknesses of the Nb_2O_5 and MgF_2 single-layer films (49.0 and 80.9 nm, respectively) were used to simulate the DBRs with two, four, and six periods, the reflective ratios calculated using Sheppard's equation with the CWave value of 450 nm were 70.0, 95.3, and 99.3%, respectively. Apparently, the reflective ratio increases with the period of the MgF_2-Nb_2O_5 bilayer films. To determine the effect of the different thicknesses of the Nb_2O_5 and MgF_2 films on the reflective properties, the actual variable n values shown in Fig. 2(a) were incorporated, with the different thicknesses of the Nb_2O_5 and MgF_2 films shown in Table 1, into the overall TMs shown in Eqs. (8)–(10) for calculations. As $d = \lambda/(4n)$ and the different thicknesses shown in Table 1 were used to calculate the CWave values of the designed DBRs with different periods, the calculated values are also shown in Table 1. As the thickness of the MgF_2 single-layer film increased from 76.9 to 84.9 nm

Table 1
Thicknesses of Nb_2O_5 and MgF_2 single-layer films used to simulate the reflectance properties of MgF_2-Nb_2O_5 DBRs. CWave: central wavelength (nm)

	Two, four, six periods					Two, four, six periods				
Nb_2O_5			49.1			45.1	47.1	49.1	51.1	53.1
MgF_2	76.9	78.9	80.9	82.9	84.9			80.9		
CWave for Nb_2O_5	450	450	450	450	450	413	431	450	468	486
CWave for MgF_2	428	439	450	461	472	450	450	450	450	450

and that of the Nb_2O_5 single-layer film was set at 49.1 nm, the corresponding CWave values increased from 428 to 472 nm. As the thickness of the Nb_2O_5 film increased from 45.1 to 53.1 nm and that of the MgF_2 film was set at 80.9 nm, the corresponding CWave values increased from 413 to 486 nm. These results suggest that the variation of the Nb_2O_5 film has a larger effect on the CWave values of the designed DBR.

The reflectance spectra determined by theoretical calculations at the light wavelengths of 300–800 nm are shown in Figs. 3–5 for the MgF_2-Nb_2O_5 bilayer films with two, four, and six periods, respectively. The simulated results of the designed DBR with CWave of 450 nm and two periods are listed in Table 2, including the MaxR value, the wavelength to obtain the maximum reflective ratio (Wave, nm), bandwidth (BD, nm, defined as the range to show 90% of the maximum reflective ratio), CWave, and full width at half-maximum (FWHM, nm). As Fig. 3 and Table 2 show, all the simulation reflectance spectra had similar trends at light wavelengths of 300–800 nm. As the thickness of the MgF_2 (Nb_2O_5) film increased from 76.9 (45.1) to 84.9 (53.1) nm and the thickness of the Nb_2O_5 (MgF_2) film was set at 49.1 (80.9) nm, the MaxR value decreased from 71.6 (70.9) to 69.3% (70.0%), the Wave value shifted from 415 (428) to 448 (443) nm, the CWave value of the designed reflector shifted from 425 (442) to 457 (453) nm, and the BD value increased from 61 (108) to 114 (113) nm. However, the FWHM values also increased with the thicknesses of the Nb_2O_5 and MgF_2 single-layer films.

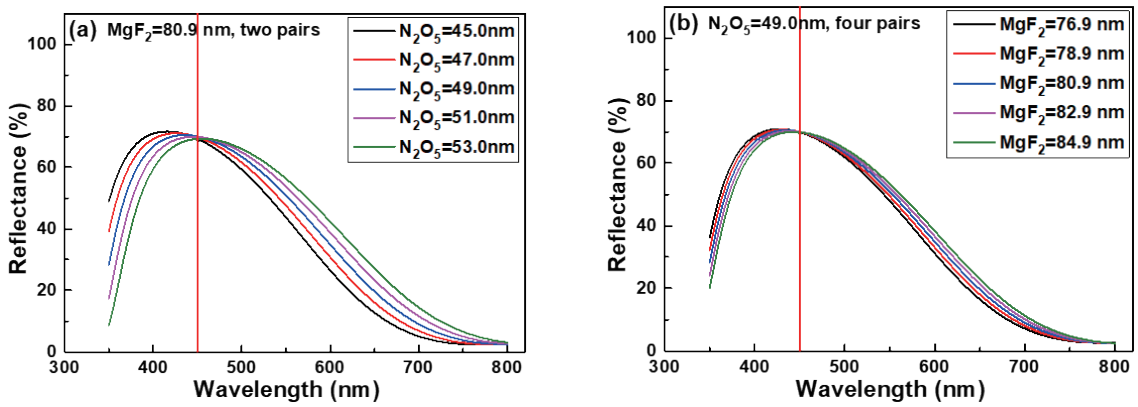

Fig. 3. (Color online) Simulated results of the designed DBR with CWave value of 450 nm and two periods. (a) The thickness of the MgF_2 film was set at 80.9 nm and that of the Nb_2O_5 film was changed from 45.0 to 53.0 nm. (b) The thickness of the Nb_2O_5 film was set at 49.0 nm and that of the MgF_2 film was changed from 76.9 to 84.9 nm.

Table 2
Simulated results of the designed DBR with CWave of 450 nm and two periods. MaxR: maximum reflective ratio (%), Wave: wavelength to present the maximum reflective ratio (nm), CWave: central wavelength (nm), BD: bandwidth (nm), FWHM: full width at half-maximum (nm).

Nb_2O_5			49.1			45.1	47.1	49.1	51.1	53.1
MgF_2	76.9	78.9	80.9	82.9	84.9			80.9		
MaxR	71.6	71.1	70.5	69.9	69.3	70.9	70.7	70.5	70.2	70.0
Wave	415	426	436	445	448	428	432	436	439	443
CWave	425	434	450	454	457	442	446	450	451	452
BD	61	107	110	112	114	108	109	110	112	113
FWHM	—	—	243	247	255	—	241	243	247	250

As Fig. 4 and Table 3 show, as the thickness of the MgF_2 (Nb_2O_5) film increased from 76.9 (45.1) to 84.9 (53.1) nm and the thickness of the Nb_2O_5 (MgF_2) film was set at 49.1 (80.9) nm, the MaxR value decreased from 96.3 (95.6) to 95.0% (95.3%), the Wave value shifted from 415 (428) to 448 (443) nm, the CWave value of the designed reflector shifted from 396 (442) to 460 (453) nm, the BD value increased from 149 (154) to 162 (159) nm, and the FWHM value increased from 203 (208) to 222 (216) nm. As Fig. 5 and Table 4 show, as the thickness of the MgF_2 (Nb_2O_5) film increased from 76.9 (45.1) to 84.9 (53.1) nm and the thickness of the Nb_2O_5 (MgF_2) film was set at 49.1 (80.9) nm, the MaxR value decreased (increased) from 97.6 (97.1) to 96.7% (97.3%), the Wave value shifted from 418 (429) to 445 (432) nm, the CWave value of the designed reflector shifted from 433 (441) to 475 (458) nm, the BD value increased from 114 (114) to 120 (119) nm, and the FWHM value increased from 153 (153) to 161 (161) nm.

The results in Figs. 3–5 suggested that as the thicknesses of the single-layer films deviated from $d = \lambda/(4n)$, the designed reflectors can also have high efficiency to reflect the incident light, but the deviation value of the film thickness has a large effect on the reflective characteristics of the designed DBRs. All the CWave values in Tables 2–4 are 450 nm, which suggests that the investigated overall TM can be used to simulate the reflective properties of the designed DBR. When the periods of the bilayer Nb_2O_5 and MgF_2 films are two, four, and six, the MaxR values obtained from Sheppard's approximate equation are 70.0, 95.3, and 99.3%, respectively. As the

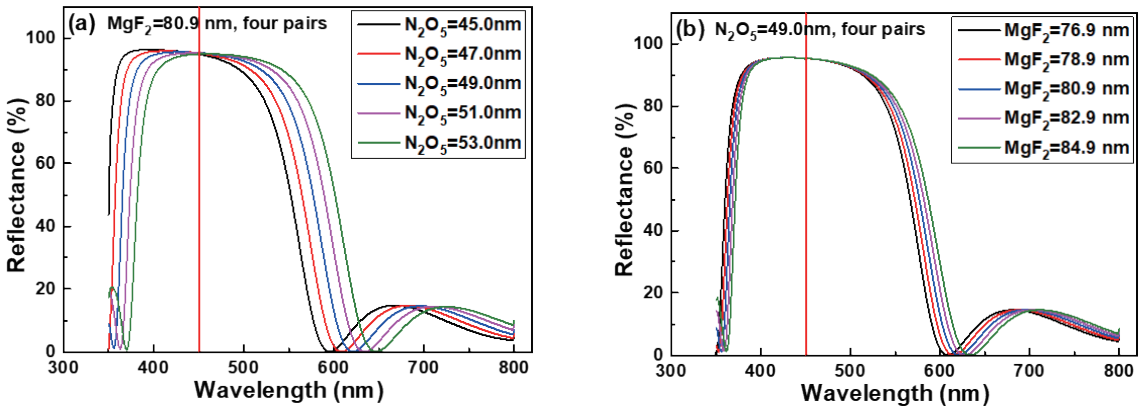

Fig. 4. (Color online) Simulated results of designed DBR with CWave value of 450 nm and four periods. (a) The thickness of the MgF_2 film was set at 80.9 nm and that of the Nb_2O_5 film was changed from 45.0 to 53.0 nm. (b) The thickness of the Nb_2O_5 film was set at 49.0 nm and that of the MgF_2 film was changed from 76.9 to 84.9 nm.

Table 3
Simulated results of designed DBR with CWave value of 450 nm and four periods. MaxR: maximum reflective ratio (%), Wave: wavelength to present the maximum reflective ratio (nm), CWave: central wavelength (nm), BD: bandwidth (nm), FWHM: full width at half-maximum (nm).

Nb_2O_5			49.1			45.1	47.1	49.1	51.1	53.1
MgF_2	76.9	78.9	80.9	82.9	84.9			80.9		
MaxR	96.3	95.9	95.5	95.2	95.0	95.6	95.6	95.5	95.5	95.3
Wave	396	414	430	445	460	429	430	430	431	432
CWave	433	444	455	465	475	450	453	455	457	459
BD	149	153	157	160	162	154	155	157	158	159
FWHM	203	207	212	217	222	208	210	212	214	216

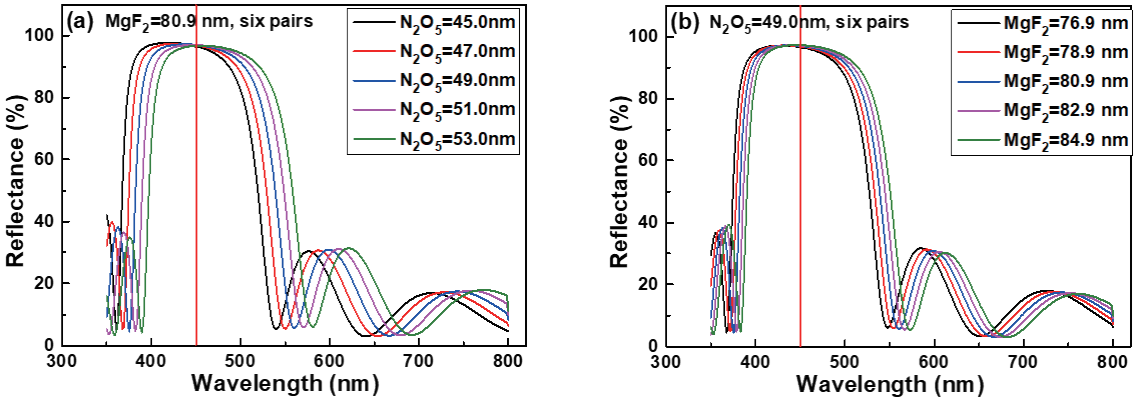

Fig. 5. (Color online) Simulated results of designed DBR with CWave value of 450 nm and six periods. (a) The thickness of the MgF_2 film was set at 80.9 nm and that of the Nb_2O_5 film was changed from 45.0 to 53.0 nm. (b) The thickness of the Nb_2O_5 film was set at 49.0 nm and that of the MgF_2 film was changed from 76.9 to 84.9 nm.

Table 4
Simulated results of designed DBR with CWave of 450 nm and six periods. MaxR: maximum reflective ratio (%), Wave: wavelength to present the maximum reflective ratio (nm), BD: bandwidth (nm), CWave: central wavelength (nm), FWHM: full width at half-maximum (nm).

Nb_2O_5			49.1			45.1	47.1	49.1	51.1	53.1
MgF_2	76.9	78.9	80.9	82.9	84.9			80.9		
MaxR	97.6	97.4	97.2	97.0	96.7	97.1	97.1	97.2	97.2	97.3
Wave	418	428	437	446	455	429	433	437	441	445
CWave	433	442	450	458	465	441	446	450	454	458
BD	114	115	117	118	120	114	116	117	118	119
FWHM	153	155	157	159	161	153	155	157	159	161

thickness of the MgF_2 (Nb_2O_5) film increased from 76.9 (45.1) to 84.9 (53.1) nm and that of the Nb_2O_5 (MgF_2) film is set at 49.1 (80.9) nm, the MaxR values slightly decrease from 96.3 (95.6) to 95.0% (95.3%). However, the MaxR values obtained from the investigated overall TM are similar to those calculated from Sheppard's approximate equation. Tables 2–4 also show that all the Wave values are smaller than the CWave values, which means that the wavelengths to present the optimum reflective ratio are smaller than the central wavelength (450 nm). When the results in Tables 3 and 4 are compared, we see that as the periods of the bilayer Nb_2O_5 and MgF_2 films increase from four to six, the BD value is reduced, and the intensity of ripples and the ripple number out of the reflective band increase.

The results in Figs. 3–5 and Tables 2–4 also show that as the deviation thickness of the single-layer film increases, the Wave and CWave values also show large changes. As the thickness of the single-layer film increases, both the Wave and CWave values decrease, and both the BD and FWHM values increase. When the CWave values in Tables 1–4 are compared, we see that as the thickness of the Nb_2O_5 film is set at 49.1 nm and that of the MgF_2 film increases from 76.9 to 84.9 nm, the CWave value obtained from $d = \lambda/(4n)$ increases from 428 to 472 nm, and the CWave value of the reflector with six periods increases from 433 to 475 nm. When the thickness of the MgF_2 film is set at 80.9 nm and that of the Nb_2O_5 film increases from 45.1 to 53.1 nm, the CWave value obtained from equation $d = \lambda/(4n)$ increases from 413 to 486 nm, and

the CWave value of the reflector with six periods increases from 429 to 432 nm. The CWave deviation values obtained from the calculated values of the investigated overall TM are smaller than those in Table 1. The reason is that the CWave deviation values in Table 1 are calculated using only the single-layer film but not the bilayer films, and the CWave deviation values in Table 4 are simulated by changing one single-layer film while keeping the other single-layer film unchanged. Therefore, the CWave deviation values obtained and presented in Table 4 are smaller than those in Table 1.

4. Conclusions

In this study, we successfully used the investigated overall TM to simulate the designed DBRS with different periods of Nb_2O_5 and MgF_2 bilayer films. The results of this study proved that even the thicknesses of the used bilayer films did not obey the derivated values from $d = \lambda/(4n)$. The reflective effect of the designed DBR still had good agreement with our requirements. The simulation results of the overall TM showed that as the thickness of one film in the bilayer structure increased while the thickness of the other film was unchanged, the maximum reflective ratio decreased slightly. When the period of the bilayer Nb_2O_5 and MgF_2 films was increased from four to six, the simulation results showed that the BD value decreased and the intensity of ripples and the ripple number out of the reflective band increased. The simulation results also showed that as the deviation thickness of the single-layer film increased, both the Wave and CWave values decreased and both the BD and FWHM values increased.

Acknowledgments

This work was supported by projects under Nos. MOST 110-2622-E-390-002 and MOST 110-2221-E-390-020.

References

1 G. J. Lee, I. Y. Hong, T. K. Kim, H. J. Park, S. K. Oh, Y. J. Cha, M. J. Park, K. J. Choi, and J. S. Kwak: Appl. Sur. Sci. **477** (2019) 220.
2 Y. S. Lee, J. H. Moon, Y. T. Moon, B. Choi, and J. T. Oh: ECS J. Solid State Sci. Technol. **9** (2020) 036002.
3 M. A. Butt, S. A. Fomchenkov, and S. N. Khonina: 3rd Int. Conf. Information Technology and Nanotechnology (ITNT, 2017).
4 T. H. Chang, T. E. Lee, N. K. Hsueh, C. H. Lin, and C. F. Yang: Microsyst. Technolog. **24** (2018) 3941.
5 J. Liu, C.Y. Lin, W. C. Tzou, N. K. Hsueh, C. F. Yang, and Y. Chen: Cryst. Growth Design **18** (2018) 5426.
6 V. Pervak, S. Naumov, G. Tempea, V. Yakovlev, F. Krausz, and A. Apolonski: Proc. SPIE **5963** (2005) 59631P.
7 J. Xu, C.H. Lin, Y.T. Chen, H.W. Tseng, P. Wang, C.F. Yang, and C.L. Lin: Sens. Mater. **33** (2021) 2619.
8 Z. S. Yuan, J. M. Jhang, P. H. Yu, C. M. Jiang, Y. C. Huang, Y. L. Wu, J. J. Lin, and C. F. Yang: Vacuum **13** (2020) 109782.
9 Y. Du, B. S. Chen, J. J. Lin, and C. F. Yang: Modern Phys. Lett. **35** (2020) 2140001.
10 K. N. Chen, C. M. Hsu, J. Liu, Y. C. Liou, and C. F. Yang: Micromachines **7** (2016) 151.
11 S. H. Woo, S. H. Kim, and C. K. Hwangbo: J. Korean Phys. Soc. **45** (2004) 99.
12 C. J. R. Sheppard: Pure and Applied Optics. J. Europ. Optical Soc. A**4** (1995) 665.
13 Y. C. Chen, C. F. Yang, and E. Y. Hsueh: J. Electrochem Soc. **157** (2010) H987.
14 H. A. Macleod: Thin-Film Optical Filters (McGraw-Hill, New York, 1985) 2nd ed.
15 F. A. Jenkins and H. E. White: Fundamentals of Optics (McGraw-Hill, Inc., 1981) 4th ed.